Theor Appl Climatol
DOI 10.1007/s00704-015-1519-6

ORIGINAL PAPER

# Estimation of daily global solar radiation as a function of routine meteorological data in Mediterranean areas

**Francisco Javier Meza**[1,2] **· María Lorenzo Yebra**[3]

Received: 3 September 2013 / Accepted: 21 May 2015


**Abstract** Solar radiation is the main responsible of many processes of the biophysical environment. Temperature changes, snow melt dynamics, carbon sequestration, evaporation from soils, plants, and open water bodies are explained by the amount of radiation received in a surface. Lack of direct observations and insufficient record length limit the ability to use global solar radiation information for resource use management and planning. Based on the general equation of Bristow and Campbell, we propose a modification that allows us to better represent atmospheric transmissivity as a function of routine meteorological variables and improve estimates of global solar radiation in Mediterranean and semi arid areas. The improved Bristow-Campbell model (IBC) is easy to use in any location where measurements of temperature, precipitation, and relative humidity are available, and present a simple solution that can be used as proxy for relative humidity in case that variable is not been measured.

## 1 Introduction

Energy received from the sun is the ultimate driver of the main ephysical, biological, and chemical processes on Earth. For instance, it is the primary energy source for photosynthesis and is the ultimate driver of the hydrological cycle (Woodwell 1967). Several studies, based on sunspot frequency and the variability provided by the elliptical path of the Earth orbit, reveal that solar activity can explain almost 30 % of recent climate variation since 1970 (Krikova and Solanski 2004). Moreover, the distance between Sun and Earth can also influence the formation of sea currents and winds, which are not only important for the development of life, but also can be used as a renewable, environmentally friendly, and secure source of energy (Salima and Chavula 2012).

Data about solar radiation is relevant for agricultural research and applications such as the estimation of reference evapotranspiration and crop water requirements for irrigation design and operation, or to assess the suitability of a cropping system by means of a crop simulation model. It is also important for energy planning, since data about solar radiation allows a correct evaluation of thermal and photovoltaic systems whose plant factors are linearly correlated with solar irradiance (Colle et al. 2001).

Measurements of global or diffuse radiation fluxes are obtained using a *pyranometer,* whereas direct radiation is measured using a *pyrheliometer* on a sun-following tracker (Georgiev et al. 2004). However, these instruments are not part of the standard meteorological station; therefore, records of solar radiation are less frequently found than those of temperature and precipitation.

Although solar radiation reaches the top of the Earth atmosphere practically undiminished (Brooks 1959), there are many conditions that alter the flux that reaches Earth surface, such as cloud cover, oceanic influence, water vapor, aerosol, and dust or smoke. Topographical effects can also be determinant, for instance the south-facing slopes on clear winter days may receive up to three times much more solar radiation than north-facing slopes in Northern Hemisphere (Klein 1977).

✉ Francisco Javier Meza
fmeza@uc.cl

[1] Centro Interdisciplinario de Cambio Global, Pontificia Universidad Católica de Chile, Santiago, Chile

[2] Departamento de Ecosistemas y Medio Ambiente. Facultad de Agronomía e Ingeniería Forestal, Pontificia Universidad Católica de Chile, Santiago, Chile

[3] Escuela Universitaria de Ingeniería Técnica Agrícola, Universidad Politécnica de Madrid (España), Madrid, Spain

Published online: 06 June 2015

Most solar radiation models rely on measured data for their development or validation, and often the uncertainty or accuracy of that measured data is unknown, so models can only be proven as good as the data employed when developing them (Myers 2005).

The geometry of the Earth and the physical laws involved allow the derivation of useful equations to predict solar radiation on clear skies (see for instance Campbell and Norman 1998), but its extension to cloudy skies is not straightforward and involves assumptions about could cover and/or type. Satellite-borne sensors can partially solve the problem allowing us to estimate cloud cover and therefore incoming short-wave radiation (Dubayah 1994); however, the length of the records and their spatial resolution are not always adequate.

There are a number of models that allow the estimation of solar radiation under a diverse range of situations, ranging from linear models based on effective sunshine hours (Angström 1924) to landscape-based models, adapted to heterogeneous topography (Coops et al. 2000), and others more appropriate for long time frames. In those models, the most commonly used independent variable is temperature (Thorton and Running 1999). Among the temperature-based models, the Bristow-Campbell model (Bristow and Campbell 1984) is the most widely used. This model relates daily variation of air temperature (difference between maximum and minimum temperature) to incoming solar radiation. Although authors provide general values for the parameters of the equation, there are examples of local calibration and adaptation to different areas or situations. For instance, Meza and Varas (2000) fitted this model to data from Chilean stations and evaluated their performance at monthly and daily level. Other models use not only information about temperature but also about precipitation, as a proxy of cloudiness, to estimate the transmittance of clear and overcast days (Bindi and Miglietta 1991). Other meteorological data, such as the ratio of atmospheric pressure at the site and at sea level, has also been used (Allen 1997), whereas others have explored the addition of local information for the calibration process using solar declination, latitude and altitude (Kilic and Öztürk 1983), and the distinction between direct and diffuse radiation on horizontal surface (Vecam 2011).

The main objective of this work is to expand the Bristow-Campbell model by incorporating additional meteorological data to describe the transmissivity parameter and apply this model to Mediterranean regions.

## 2 Materials and methods

### 2.1 Climatic and global solar radiation data

We selected 44 locations that represent a typical Mediterranean climate using the classification developed by Wladimir Köppen in 1900. This system, based on a large global data set of mean monthly precipitation and temperature values, has been updated many times, adapting the spatial distribution of the different categories to both data availability and computing power. However, recent research efforts are trying to improve this classification, especially to better discriminate areas that satisfy both the Cs and Cw criteria simultaneously (Peel et al. 2007). According to the latest Köppen-Geiger Climate classification, Mediterranean areas correspond to Csa and Csb categories, where C type climates have warm to hot summer temperatures, mild winters, and the coldest month has an average temperature between 18 °C and −3 °C. Csa and Csb correspond to Interior and Coastal Mediterranean areas, respectively. Table 1 presents geographical location and general information about each station.

The selected locations belong to the following countries: USA, Chile, Spain, France, Italy, South Africa, and Australia. Data for USA was obtained from the network of the Remote Automatic Weather Stations (RAWS), formed by 1850 solar-powered units that gather important weather information via satellite on an hourly basis. The *Dirección Meterorológica de Chile* (DMC) provides daily meteorological reports and also offers semiannual daily solar radiation bulletins. In the case of Australia, the data is provided by the Climate Data Online (CDO) service of the Australian Government Bureau of Meteorology that provides access to a range of statistics, historical weather observations, climatology maps, and other Australian climate information.

For the remaining countries (Spain, France, Italy and South Africa), the information about solar radiation was obtained from Solar Radiation Data (SODA), a website that gathers information from NASA's Surface Meteorology and Solar Energy (NASA-SSE) and HelioClim-1 Database (HC-1). NASA-SSE data set is formulated from NASA satellite, reanalysis-derived insolation, and meteorological data; HC-1 includes daily irradiation values over a horizontal plane estimated from Meteosat images. With the exception of Spain, meteorological information was obtained from the National Oceanic and Atmospheric Administration Climatic Data Center (NOAA-NCDC), the world's largest climate data archive from not only land-based stations but also from ships, buoys, weather balloons, radars, satellites, and even sophisticated weather and climate models. Spanish meteorological information was obtained from the *Banco Nacional de Datos Climatológicos de la Agencia Estatal de Meteorología* (AEMET) that compiles the historical data of the meteorological Spanish records.

### 2.2 Global solar radiation models

Bristow and Campbell (1984) stated that the difference between the maximum and minimum temperature in a

**Table 1** Geographic location and main data characteristics of selected stations

| Country | Location | Lat (°N) | Long (°E) | Years of record | Humidity |
|---|---|---|---|---|---|
| Australia | Adelaide | −34.55 | 138.36 | 20 | No |
| Australia | Esperance | −33.85 | 121.54 | 20 | No |
| Australia | Geraldton | −28.77 | 114.60 | 20 | No |
| Australia | Melbourne | −37.47 | 144.57 | 20 | No |
| Australia | Moruya Heads | −35.90 | 135.00 | 20 | No |
| Australia | Perth | −31.57 | 115.52 | 20 | No |
| Australia | Portland | −38.34 | 141.60 | 20 | No |
| Australia | Sydney | −33.86 | 151.21 | 20 | No |
| Chile | Concepcion | −36.70 | −74.55 | 5 | Yes |
| Chile | Curico | −34.92 | −71.20 | 5 | Yes |
| Chile | La Platina | −33.59 | −71.00 | 5 | Yes |
| Chile | Portezuelo | −36.51 | −72.58 | 5 | Yes |
| Chile | Pudahuel | −33.23 | −70.40 | 6 | Yes |
| Chile | Sauzal | −35.52 | −72.11 | 5 | Yes |
| Chile | Temuco | −38.60 | −72.40 | 5 | Yes |
| France | Montpellier | 43.70 | 3.87 | 22 | No |
| France | Nice | 43.60 | 7.12 | 22 | No |
| France | Perpignan | 42.73 | 2.89 | 22 | No |
| Italy | Cagliari | 39.21 | 9.30 | 15 | No |
| Italy | Florence | 43.80 | 11.15 | 15 | No |
| Italy | Naples | 40.83 | 14.27 | 15 | No |
| Italy | Palermo | 38.11 | 13.36 | 15 | No |
| Italy | Rome | 41.90 | 12.50 | 15 | No |
| Spain | Almeria | 36.83 | 2.30 | 15 | No |
| Spain | Barcelona | 41.38 | 2.90 | 15 | No |
| Spain | Caceres | 39.48 | −6.30 | 15 | No |
| Spain | Ciudad Real | 38.98 | −3.55 | 15 | No |
| Spain | Cordoba | 37.88 | −4.50 | 15 | No |
| Spain | Jerez | 36.68 | −6.10 | 15 | No |
| Spain | Madrid | 40.40 | −3.70 | 15 | No |
| Spain | Mallorca | 39.56 | 2.39 | 15 | No |
| Spain | Melilla | 35.31 | −2.95 | 15 | No |
| Spain | Tenerife | 28.45 | −16.17 | 15 | No |
| Spain | Tortosa | 40.80 | 0.51 | 15 | No |
| Spain | Valencia | 39.46 | −0.37 | 15 | No |
| USA | Cedarville | 41.58 | −120.17 | 25 | Yes |
| USA | Corvallis | 44.56 | −123.25 | 25 | Yes |
| USA | Creston | 48.18 | −120.52 | 25 | Yes |
| USA | Fallon | 39.56 | −90.69 | 25 | Yes |
| USA | Forth Collins | 40.45 | −105.57 | 25 | Yes |
| USA | Odessa | 47.33 | −102.39 | 25 | Yes |
| USA | Tucson | 32.16 | −110.88 | 25 | Yes |
| USA | Twin Falls | 42.56 | −114.41 | 25 | Yes |

day depends on Bowen ratio as sensible heat is mainly driven by solar radiation and is responsible of the variations of the temperature. In this way, Bristow and Campbell (1984) proposed the estimation of the ratio between Global Solar radiation and solar radiation at the top of the atmosphere ($R_{\mathrm{Gest}}/R_{\mathrm{A}}$) as a function of the difference of maximum and minimum temperatures ($\Delta T$, °C).

The equation proposed for the Bristow-Campbell model (BC model) was as follows:

$$\frac{R_{\mathrm{Gest}}}{R_{\mathrm{A}}} = A\left[1-\exp\left(-B\Delta T^{C}\right)\right] \tag{1}$$

In this expression, all three constants ($A$, $B$, and $C$) have a physical meaning. $A$ is the maximum radiation expected on a clear day, being distinctive for each location and depending on air quality and altitude. $B$ and $C$ control the rate in which the increase of temperature influences solar radiation, approaching to the limit set by the parameter A.

This simple model neglects other factors that affect the amount of solar radiation that reaches the Earth's surface, such as relative humidity, cloud cover, etc. A more comprehensive model should be able to represent in an explicit manner the impact of other meteorological variables. For instance, an improved model should be able to represent the ratio between global solar radiation and radiation at the top of the atmosphere ($R_{\mathrm{Gest}}/R_{\mathrm{A}}$) as a function of maximum temperature ($T_M$, °C), minimum temperature ($T_m$, °C), occurrence of precipitation (OPp, binary value) since this binary variable is a valid proxy for cloud cover, and relative humidity (*RH;* dimensionless) or vapor pressure deficit (*VPD*) as it is related to atmospheric transmissivity. Comparatively, the latter variable is less frequently recorded, but when available, it can improve the precision of the estimation of solar radiation.

Here, we suggest a model that maintains the functional form to represent the effect of solar radiation on diurnal temperature range (i.e., the difference between maximum and minimum temperature), but adds flexibility to the parameter that reflects atmospheric transmissivity ($A$).

The equation proposed for an improved Bristow-Campbell model (IBC model) is as follows:

$$\frac{R_{\mathrm{Gest}}}{R_{\mathrm{A}}} = \left(b_0 + b_1 \sin(M) + b_2 \cos(M) + b_3\,\mathrm{RH} + b_4\,\mathrm{OPp}\right) \times \left[1-\exp\left(-b_5 (T_{\mathrm{M}}-T_{\mathrm{m}})^{b_6}\right)\right] \tag{2}$$

with $M = \frac{2\pi j}{365}$ and $j$ as the Julian day. The parameters associated to sine and cosine functions allow the function to change seasonally according to a Fourier series.

Even though this model incorporates more variables that influence solar global radiation, there are still many unconsidered factors that may alter the flux of solar radiation that reaches Earth surface, such as pollution, local effects of the marine influence above the temperature, or elevation of the station.

Radiation at the top of the atmosphere ($R_{\mathrm{A}}$, MJ m$^{-2}$ day$^{-1}$) is calculated for any location as a function of the distance and the mean distance from the Sun to Earth ($d$ and $d_{\mathrm{m}}$, km), latitude ($\Phi$, rad), solar declination ($\delta$, rad), and solar angle at sunset ($H_s$, rad) using the following expression (Romo and Arteaga 1983):

$$R_{\mathrm{A}} = 37.54 \times \left(\frac{d_m}{d}\right)^2 \times \left[(H_s)\sin\Phi\sin\delta + \cos\Phi\cos\delta\sin H_{\mathrm{s}}\right] \tag{3}$$

The mean distance between Sun and Earth ($d_{\mathrm{m}}/d$), also known as the correction factor for the distance Sun-Earth ($\rho^2$), can be calculated using the following equation (Spencer 1971):

$$\rho^2 = \left(\frac{d_m}{d}\right)^2 = 1.000110 + 0.034221\cos\Gamma + 0.034221\sin\Gamma + 0.000719\cos2\Gamma + 0.000077\sin2\Gamma \tag{4}$$

This expression uses the daily angle ($\Gamma$, rad) as a function of the Julian day ($j$):

$$\Gamma = \frac{2\Pi}{365} \times (j-1) \tag{5}$$

The solar angle at sunset ($H_s$) is computed using the equation:

$$H_s = \cos^{-1}(-\tan\Phi \times \tan\delta) \tag{6}$$

and solar declination ($\delta$) is calculated with the following expression:

$$\delta = \frac{23.5}{57.3} \times \sin\left(\frac{284 + j}{365} \times 2\pi\right) \tag{7}$$

Some stations do not record relative humidity (Table 1). For those cases, one can omit this variable so that the fitted parameters associated to the rest of the variables will change according to the particular correlation structure they have with the missing relative humidity variable. In this case, we have developed a different strategy to deal with missing relative humidity values. Given the fact that in many climate types, especially in Mediterranean environments, the dew point temperature and the minimum temperature are very similar, one can estimate actual vapor pressure as

$$e_{\mathrm{a}} = 6.11\exp\left(\frac{17.27T_{\mathrm{m}}}{237.3 + T_{\mathrm{m}}}\right) \tag{8}$$

We can estimate the saturated vapor pressure at the mean temperature as

$$e_{\mathrm{s}} = 6.11\exp\left(\frac{17.27\left(\frac{T_{\mathrm{m}} + T_{\mathrm{M}}}{2}\right)}{237.3 + \left(\frac{T_{\mathrm{m}} + T_{\mathrm{M}}}{2}\right)}\right) \tag{9}$$

If we assume that the actual vapor pressure does not change during the day, the estimation of mean relative humidity will be obtained as the ratio of Eqs. 8 and 9 expressed as percentage.

$$RH = \frac{e_a}{e_s}100 \tag{10}$$

### 2.3 Parameter estimation

Values of the constants $A$, $B$, and $C$ in the BC model and $b_0$ to $b_6$ in the IBC model were obtained by minimizing the sum of the squared errors, calculated as

$$E = \sum \left( \frac{R_G}{R_A} - \frac{R_{Gest}}{R_A} \right)^2 \tag{11}$$

Three independent equations ($gi$) for the case of the BC model and seven equations ($fi$), one for each parameter in Eq. 2, for the case of the IBC model were obtained by taking partial derivatives of the sum of squared errors and forcing them to be equal to zero. Mathematically, the expressions correspond to

$$g_1 = \frac{\partial E}{\partial A} = 0; \, g_2 = \frac{\partial E}{\partial B} = 0; \, g_3 = \frac{\partial E}{\partial C} = 0; \, f_i = \frac{\partial E}{\partial b_i} = 0, \quad i = 0, 1, \ldots, 6 \tag{12}$$

These derivatives are calculated numerically using finite differences. We then used a Newton–Raphson algorithm for multivariate nonlinear optimization. To avoid numerical errors and inconsistent solutions, it is advisable to apply some restrictions such as non-negativity for the $b_0$ and $b_6$ coefficients. The procedure can be easily implemented using *Solver* application of the Excel software.

## 3 Results and discussion

### 3.1 BC model

Because global solar radiation is primarily driven by the amount of energy that reaches the top of the atmosphere, we calculated the determination coefficient ($R^2$) between these two variables and use it as a first benchmark to judge whether the BC model or the IBC model improved the estimations of global solar radiation. Mean value of the determination coefficient was of 0.628 with a standard deviation of 0.2.

Table 2 shows the results of the parameters estimated minimizing the sum of the squared errors for the BC model, root mean squared error, determination coefficient of the BC and IBC model, and their respective Akaike information criterion (AIC). The latter allow us to judge if the model with more parameters (IBC model) is justified as the AIC balances the addition of parameters and the reduction in the mean squared error.

BC model shows good results in comparison to a simple linear model based on solar radiation at the top of the atmosphere. The determination coefficient increases in all stations with an average of 0.12 and in some stations increasing more than 0.25. Only one station (Firenze) shows a reduction in this value (0.01).

As it has been proved by other authors (e.g., Meza and Varas 2000), the BC model performs well and allows us to capture a substantial part of the variability in global solar radiation.

### 3.2 IBC model

The Bristow-Campbell model has two main components, one that describes the sensitivity of the system to changes in temperature, represented by the $B$ and $C$ coefficients in Eq. 1 and the coefficient that represents the transmissivity of the atmosphere ($A$). We proposed an improvement in the BC model including other common climate variables that will allow us to better represent the variability of transmissivity. Due to the nonlinear nature of the functions used, it was necessary to recalibrate all parameters and rename them as b coefficients (b0 to b6). Table 3 shows the parameters obtained after minimizing of the sum of squared errors. In addition, a determination coefficient, root mean squared error, and AIC are also presented.

The IBC model showed better results. Determination coefficient increased from a mean value of 0.768 to 0.814 in the case of the IBC model. Consequently, the RMSE decreased from 3.78 to 3.41 (MJ $m^{-2}$ $day^{-1}$). AIC values experienced a reduction so we can conclude that a more sophisticated model with more parameters is justified when climate records of precipitation and relative humidity are present. Even in the case where there are no records of relative humidity, the use of an alternative solution (Eqs. 8 to 10) produced reasonable good results and improved the estimation of global solar radiation. Values of relative humidity estimated are only a proxy to the real relative humidity values and may not be used in other context than in the one proposed here to refine the estimations of global solar radiation.

Another important feature of the IBC model is that it reduces bias in the estimation of solar radiation. Figure 1 shows a panel of four different stations comparing the results applying the BC and IBC model. The equation that describes observed vs estimated data is shown in the upper corner of each graph. In all cases, the intercept of this equation (bias estimation) is reduced substantially.

In the IBC model, coefficients associated to the Fourier series ($b_1$ and $b_2$) are almost always significantly different than zero. The inclusion of these values allows us to account for

**Table 2** Parameters of the Bristow-Campbell model and goodness of fit statistics for the stations considered in the study

| Country | Station Name | $R^2$ ($R_A$ $R_G$) | *A* | *B* | *C* | RMSE (MJ m$^{-2}$ day$^{-1}$) | $R^2$ | AIC |
|---|---|---|---|---|---|---|---|---|
| Australia | Adelaide | 0.576 | 0.807 | 0.366 | 0.593 | 5.139 | 0.661 | 47178 |
| Australia | Esperance | 0.581 | 0.688 | 0.207 | 1.081 | 4.393 | 0.716 | 44755 |
| Australia | Geraldton | 0.729 | 0.727 | 0.203 | 1.041 | 3.505 | 0.800 | 41270 |
| Australia | Melbourne | 0.503 | 0.679 | 0.135 | 1.161 | 5.189 | 0.652 | 47327 |
| Australia | Moruya Heads | 0.306 | 0.734 | 0.036 | 1.515 | 2.525 | 0.902 | 36205 |
| Australia | Perth | 0.705 | 0.795 | 0.099 | 1.116 | 3.591 | 0.831 | 41646 |
| Australia | Portland | 0.154 | 0.723 | 0.289 | 0.701 | 7.650 | 0.196 | 53318 |
| Australia | Sydney | 0.437 | 0.670 | 0.072 | 1.718 | 4.426 | 0.690 | 44871 |
| Chile | Concepcion | 0.005 | 0.596 | 0.029 | 1.594 | 7.892 | 0.124 | 10685 |
| Chile | Curico | 0.656 | 0.631 | 0.011 | 1.941 | 2.474 | 0.900 | 7131 |
| Chile | La Platina | 0.746 | 0.646 | 0.004 | 2.313 | 2.319 | 0.921 | 5327 |
| Chile | Portezuelo | 0.763 | 0.717 | 0.007 | 2.131 | 3.024 | 0.902 | 8311 |
| Chile | Pudahuel | 0.795 | 0.687 | 0.030 | 1.555 | 2.617 | 0.914 | 9836 |
| Chile | Sauzal | 0.746 | 0.713 | 0.011 | 1.938 | 2.702 | 0.917 | 8502 |
| Chile | Temuco | 0.112 | 1.649 | 0.020 | 1.077 | 5.242 | 0.575 | 9431 |
| France | Montpellier | 0.630 | 0.819 | 0.066 | 1.224 | 3.983 | 0.779 | 44816 |
| France | Nice | 0.658 | 0.677 | 0.057 | 1.857 | 4.404 | 0.729 | 46425 |
| France | Perpignan | 0.601 | 1.090 | 0.135 | 0.706 | 3.911 | 0.718 | 44527 |
| Italy | Cagliari | 0.692 | 0.689 | 0.082 | 1.312 | 3.761 | 0.779 | 28010 |
| Italy | Firenze | 0.740 | 0.649 | 0.403 | 1.242 | 4.742 | 0.730 | 30375 |
| Italy | Napoli | 0.674 | 0.699 | 0.058 | 1.655 | 4.391 | 0.746 | 46371 |
| Italy | Palermo | 0.731 | 0.678 | 0.330 | 1.144 | 4.343 | 0.747 | 29182 |
| Italy | Roma | 0.776 | 0.725 | 0.124 | 1.228 | 3.782 | 0.815 | 43982 |
| Spain | Almeria | 0.770 | 0.692 | 0.057 | 1.950 | 3.371 | 0.815 | 27984 |
| Spain | Barcelona | 0.632 | 0.643 | 0.072 | 1.716 | 4.023 | 0.736 | 44978 |
| Spain | Caceres | 0.725 | 0.790 | 0.043 | 1.458 | 2.813 | 0.894 | 39253 |
| Spain | Ciudad Real | 0.716 | 0.724 | 0.033 | 1.632 | 2.970 | 0.871 | 40120 |
| Spain | Cordoba | 0.725 | 0.734 | 0.036 | 1.515 | 2.525 | 0.902 | 36205 |
| Spain | Jerez | 0.798 | 0.763 | 0.110 | 1.222 | 2.990 | 0.869 | 40228 |
| Spain | Madrid | 0.724 | 0.877 | 0.074 | 1.138 | 2.862 | 0.876 | 39531 |
| Spain | Mallorca | 0.746 | 0.767 | 0.113 | 1.157 | 3.527 | 0.822 | 42872 |
| Spain | Melilla | 0.736 | 0.713 | 0.430 | 1.000 | 3.713 | 0.777 | 43697 |
| Spain | Tenerife | 0.532 | 0.666 | 0.563 | 0.919 | 4.033 | 0.564 | 45016 |
| Spain | Tortosa | 0.647 | 0.776 | 0.064 | 1.271 | 3.455 | 0.801 | 42541 |
| Spain | Valencia | 0.696 | 0.670 | 0.058 | 1.719 | 3.235 | 0.822 | 41489 |
| USA | Cedarville | 0.758 | 0.789 | 0.082 | 1.159 | 3.184 | 0.870 | 46714. |
| USA | Corvallis | 0.734 | 0.870 | 0.075 | 0.988 | 3.053 | 0.877 | 45998 |
| USA | Creston | 0.681 | 0.788 | 0.061 | 1.146 | 3.396 | 0.855 | 47571 |
| USA | Fallon | 0.799 | 0.847 | 0.096 | 0.978 | 2.943 | 0.879 | 25032 |
| USA | Fort Collins | 0.521 | 0.709 | 1.272 | 0.028 | 4.918 | 0.521 | 27813 |
| USA | Odessa | 0.775 | 0.736 | 0.039 | 1.419 | 2.973 | 0.889 | 44352 |
| USA | Tucson | 0.680 | 0.801 | 0.038 | 1.433 | 2.961 | 0.826 | 42067 |
| USA | Twin Falls | 0.751 | 0.743 | 0.112 | 1.066 | 3.615 | 0.828 | 47811 |

seasonal variations in the atmospheric transmissivity. Because of the different solar elevation angle during the year, in winter, the optical mass is greater so the attenuation of the solar radiation is higher (following the Beer´s Law); the opposite is true during summer as the solar declination angle is closer to the stations latitude.

**Table 3** Parameters of the improved Bristow-Campbell model and goodness of fit statistics for the stations considered in the study

| Station name | $b_0$ | $b_1$ | $b_2$ | $b_3$ | $b_4$ | $b_5$ | $b_6$ | RMSE (MJ m$^{-2}$ day$^{-1}$) | $R^2$ | AIC |
|---|---|---|---|---|---|---|---|---|---|---|
| Adelaide | 0.954 | −0.102 | 0.000 | −0.453 | −0.032 | 0.529 | 0.904 | 4.648 | 0.723 | 45635 |
| Esperance | 0.827 | −0.053 | 0.018 | −0.265 | −0.052 | 0.181 | 1.407 | 4.187 | 0.742 | 44021 |
| Geraldton | 0.869 | −0.001 | 0.035 | −0.296 | −0.037 | 0.114 | 1.618 | 3.383 | 0.814 | 40730 |
| Melbourne | 0.839 | −0.088 | −0.009 | −0.302 | −0.077 | 0.146 | 1.377 | 4.829 | 0.699 | 46225 |
| Moruya Heads | 0.509 | −0.124 | −0.044 | 0.237 | −0.061 | 0.067 | 1.714 | 5.129 | 0.600 | 47156 |
| Perth | 0.849 | −0.001 | 0.040 | −0.214 | −0.062 | 0.145 | 1.110 | 3.469 | 0.842 | 41120 |
| Portland | 0.795 | −0.184 | −0.260 | 0.182 | −0.112 | 0.287 | 0.646 | 6.410 | 0.435 | 50595 |
| Sydney | 0.751 | 0.015 | 0.032 | −0.101 | −0.083 | 0.078 | 1.723 | 4.262 | 0.713 | 44295 |
| Concepcion | 1.080 | 0.041 | −0.384 | −0.511 | −0.122 | 0.072 | 1.394 | 6.153 | 0.468 | 9930 |
| Curico | 0.799 | 0.007 | −0.053 | −0.358 | −0.084 | 0.020 | 1.786 | 2.277 | 0.915 | 6884 |
| La Platina | 0.586 | 0.004 | 0.044 | 0.094 | −0.002 | 0.006 | 2.088 | 2.236 | 0.926 | 5250 |
| Portezuelo | 0.992 | 0.000 | −0.034 | −0.482 | −0.057 | 0.013 | 2.005 | 2.647 | 0.925 | 7876 |
| Pudahuel | 0.721 | −0.012 | 0.047 | −0.246 | −0.088 | 0.067 | 1.362 | 2.298 | 0.934 | 9308 |
| Sauzal | 0.586 | 0.004 | 0.044 | 0.094 | −0.002 | 0.006 | 2.088 | 2.236 | 0.926 | 5250 |
| Temuco | 1.216 | 0.086 | −0.178 | −0.777 | −0.105 | 0.146 | 0.816 | 4.583 | 0.675 | 9027 |
| Montpellier | 0.876 | −0.066 | −0.053 | −0.030 | −0.102 | 0.092 | 1.039 | 3.761 | 0.803 | 44056 |
| Nice | 0.728 | 0.058 | −0.031 | −0.030 | −0.160 | 0.101 | 1.511 | 4.006 | 0.776 | 45070 |
| Perpignan | 0.888 | −0.028 | 0.033 | 0.314 | −0.208 | 0.135 | 0.724 | 3.692 | 0.749 | 43758 |
| Cagliari | 0.688 | −0.033 | −0.055 | −0.038 | −0.178 | 0.207 | 0.968 | 2.621 | 0.893 | 24330 |
| Firenze | 0.675 | −0.030 | −0.068 | −0.047 | −0.191 | 0.664 | 1.133 | 4.019 | 0.806 | 28694 |
| Napoli | 0.844 | −0.111 | −0.047 | −0.259 | −0.109 | 0.170 | 1.385 | 3.542 | 0.835 | 42945 |
| Palermo | 0.547 | −0.014 | −0.049 | 0.144 | −0.167 | 0.557 | 0.944 | 3.060 | 0.874 | 25653 |
| Roma | 0.960 | −0.021 | −0.063 | −0.451 | −0.115 | 0.320 | 1.113 | 3.445 | 0.846 | 42498 |
| Almeria | 0.692 | −0.002 | −0.031 | −0.010 | −0.153 | 0.086 | 1.789 | 3.040 | 0.849 | 26892 |
| Barcelona | 0.249 | 0.050 | 0.060 | 0.688 | −0.211 | 0.101 | 1.365 | 3.444 | 0.807 | 42640 |
| Caceres | 0.910 | 0.001 | 0.024 | −0.166 | −0.162 | 0.092 | 1.185 | 2.558 | 0.912 | 37871 |
| Ciudad Real | 0.781 | −0.005 | 0.009 | −0.085 | −0.150 | 0.066 | 1.410 | 2.671 | 0.896 | 38560 |
| Cordoba | 0.864 | −0.003 | 0.013 | −0.245 | −0.119 | 0.074 | 1.332 | 2.490 | 0.905 | 32897 |
| Jerez | 0.920 | 0.001 | −0.018 | −0.318 | −0.120 | 0.233 | 1.125 | 2.810 | 0.884 | 39247 |
| Madrid | 0.714 | −0.002 | 0.082 | 1.155 | −0.292 | 0.053 | 0.959 | 2.577 | 0.899 | 37988 |
| Mallorca | 0.886 | 0.015 | 0.005 | −0.257 | −0.146 | 0.199 | 1.121 | 3.234 | 0.851 | 41631 |
| Melilla | 0.823 | 0.027 | −0.022 | −0.157 | −0.170 | 0.589 | 1.010 | 3.209 | 0.833 | 41509 |
| Tenerife | 0.302 | 0.098 | 0.069 | 0.686 | −0.044 | 0.417 | 0.662 | 3.443 | 0.682 | 42637 |
| Tortosa | 0.695 | 0.033 | 0.017 | 0.105 | −0.176 | 0.090 | 1.192 | 3.098 | 0.840 | 40941 |
| Valencia | 0.979 | −0.008 | −0.041 | −0.469 | −0.155 | 0.116 | 1.601 | 2.752 | 0.871 | 39044 |
| Cedarville | 0.837 | 0.020 | 0.008 | −0.002 | −0.100 | 0.134 | 1.064 | 2.992 | 0.885 | 45643 |
| Corvallis | 0.948 | 0.016 | −0.005 | −0.354 | −0.056 | 0.110 | 0.999 | 2.862 | 0.892 | 44835 |
| Creston | 1.008 | 0.028 | 0.013 | −0.409 | −0.056 | 0.092 | 1.066 | 3.209 | 0.871 | 46560 |
| Fallon | 0.888 | −0.018 | 0.004 | −0.187 | −0.108 | 0.186 | 0.794 | 2.796 | 0.891 | 24527 |
| Fort Collins | 1.319 | −0.031 | −0.018 | −0.848 | −0.081 | 0.801 | 0.088 | 3.836 | 0.709 | 25526 |
| Odessa | 0.822 | −0.005 | 0.037 | −0.210 | −0.096 | 0.063 | 1.342 | 2.751 | 0.905 | 42992 |
| Tucson | 0.831 | −0.011 | 0.060 | −0.126 | −0.077 | 0.036 | 1.568 | 2.720 | 0.853 | 40647 |
| Twin Falls | 0.899 | 0.003 | 0.014 | −0.372 | −0.068 | 0.232 | 0.944 | 3.319 | 0.855 | 46800 |

As expected, the increase in relative humidity and consequently vapor pressure reduces atmospheric transmissivity; on average, an increase in relative humidity of 0.1 reduces atmospheric transmissivity by 0.01.

The occurrence of precipitation also reduces atmospheric transmissivity. During rainy days (OPp=1), the value of this coefficient is reduced by 0.1 on average. In the BC model, the effect of cloudy skies was indirectly captured by the reduction

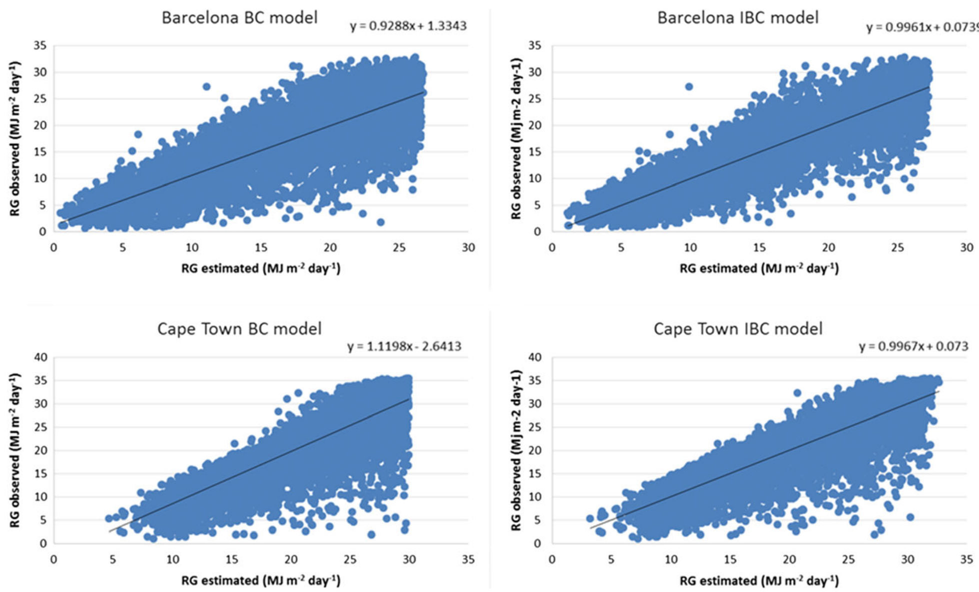


**Fig. 1** Comparison between observed and estimated global solar radiation using the BC and IBC models

of maximum temperature and increase in minimum temperature observed in rainy days. Nevertheless, a more explicit representation of this effect in the IBC model produces better results in the estimation of global solar radiation.

One additional factor that can be considered to improve the estimations of solar global radiation is the altitude of the station. Solar radiation that reaches the Earth's surface is influenced by altitude above sea level due to the diminishing of the layer of air upon it. As a result, with the same meteorological conditions, higher locations receive more global solar radiation than at sea level.

Air quality affects the amount of solar radiation that reaches the surface. Stations located in areas of high pollution (nearby great urban centers) tend to have lower values of atmospheric transmissivity. Because of the dynamic nature of this phenomenon, it is advisable to recalibrate the IBC model every 5 to 10 years.

### 3.3 Sensitivity of parameters to record length

Parameter fitting highly depends on data characteristics. The IBC model shows that incorporating more variables to better describe atmospheric transmissivity improves the precision of the estimates of global solar radiation. Data quality and accessibility is an important aspect; typical exploratory data analysis techniques will be sufficient to detect and remove outliers.

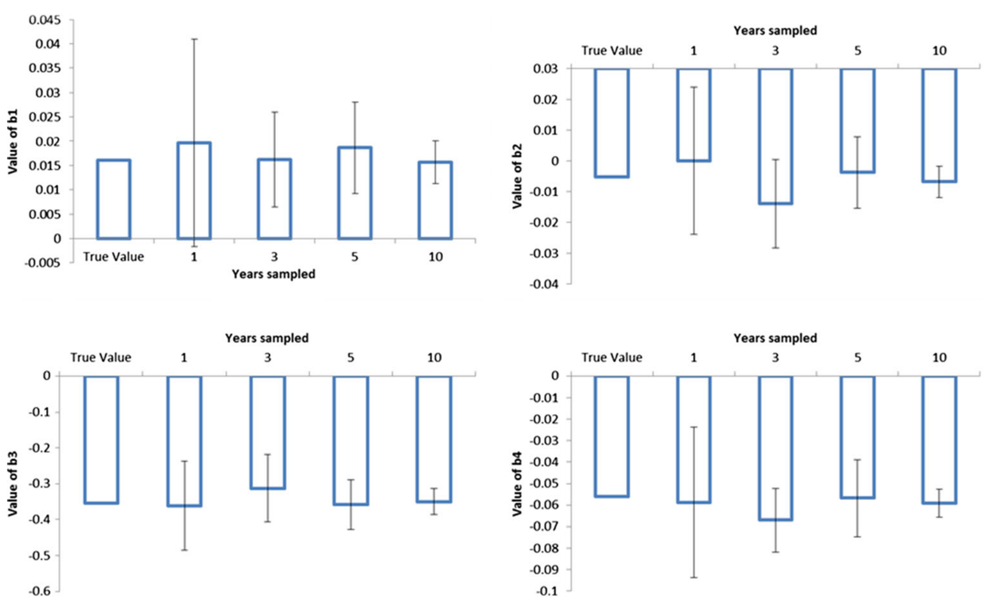


**Fig. 2** Sensitivity of IBC model parameters in the Corvallis station as a function of the number of years used in the calibration procedure. *Error bars* represent standard deviations obtained from ten replicates

In this work, we were interested in a different but related subject, which is sensitivity of parameter estimation to record length. To study the sensitivity of the parameters to sample size, we used the Corvallis station that has 25 years of daily meteorological records. We applied a resampling procedure to randomly select 10 subsets of 1, 3, 5, and 10 years of daily meteorological variables and fit the parameters of the IBC model. Some parameters, like the coefficients $b_0$ and $b_6$ in Eq. 2, are very stable and can be estimated with sufficient confidence using small sample sizes. Figure 2 shows the behavior of the mean estimates as a function of the number of years sampled. The coefficients associated to the Fourier series that describe seasonal variation are quite sensitive and require a substantially large number of years with daily meteorological values to stabilize (10 years). Coefficients associated to relative humidity and the occurrence of precipitation are less sensitive, and require a rather small number of years (between 3 and 5). In the case of the coefficient that describes the influence of clouds via precipitation occurrence, the number of years to produce a reasonable estimate will depend on the climatic regime. In semi-arid and dry Mediterranean areas, it will be advisable to have a large sample because rainfall events are less frequent, especially in spring and summer months.

## 4 Conclusions

In this work, we proposed an improved model for the estimation of global solar radiation. Starting from the work of Bristow and Campbell (1984), we developed an equation that includes other relevant meteorological variables to better represent the variability on atmospheric transmissivity. The IBC model shows very good results and outperforms the BC model even when only a proxy of relative humidity is used.

Those stations influenced by the proximity of the sea have less reliable results when applying the model with daily information, especially when no information about relative humidity was available.

With the exception of Chile, USA, and Australia, the information for the rest of the countries was collected from two different sources. Finding stations from both agencies as close as possible was a priority, but information about altitude in one of networks was not provided, being impossible to determine if the differences in position and height were the cause if the unreliable results.

Mean values of the constants included in the model can be calculated in order to elaborate a general equation that could be applied in Mediterranean area. However, the coefficients associated to seasonal variation of the atmospheric transmissivity need to be calibrated locally to account for specific regimes and differences between southern and northern hemisphere and coastal and inland areas.

Further research is needed to validate the IBC model in other type of environments where thermal amplitude is less influenced by global solar radiation such as tropical and humid climates.

**Acknowledgments** This work has been supported by FONDECYT grant 1120713. María Lorenzo would like to thank Jose Luis Rodriguez Gil (University of Guelph) for valuable advice and revision of an early version of this manuscript.

## References

Allen R (1997) Self-calibrating method for estimating solar radiation from air temperature. J Hydrol Eng 2:56–57

Angström A (1924) Solar and terrestrial radiation. QJR Meteorol Soc 50: 121–125

Bindi M, Miglietta F (1991) Estimating daily global radiation from air temperature and rainfall measurements. Clim Res 1:117–124

Bristow K, Campbell G (1984) On the relationship between incoming solar radiation and daily maximum and minimum temperature. Agric For Meteorol 31:159–166

Brooks FA (1959) An introduction of physical microclimatology. Univ. of California, Davis, p 264

Campbell SG, Norman JL (1998) An introduction to environmental biophysics, 2nd edn. Springer, New York

Colle S, De Abreu SL, Ruther R (2001) Uncertainty in economic analysis of solar water heating and photovoltaic systems. Sol Energy 70(2):131–142

Coops NC, Waring RH, Moncrieff JB (2000) Estimating mean monthly incident solar radiation on horizontal and inclined slopes from mean monthly temperatures extremes. Int J Biometeorol 44:204–211

Dubayah RC (1994) Modeling a solar radiation topo-climatology for the Rio Grande River basin. J Veg Sci 5:627–640

Georgiev A, Roth P, Olivares A (2004) Sun following system adjustment at the UTFSM. Energ Convers Manage 45: 1795–1806

Kilic A, Öztürk A (1983) Güneş Enerjisi. Kipaş Dağıtımcılık, İstanbul

Klein SA (1977) Calculation of monthly average insolation on tilted surfaces. Sol Energy 19:325–329

Krikova NA, Solanski SK (2004) Solar variability and global warming: a statistical comparison since 1850. Adv Space Res 34:361–364

Meza F, Varas E (2000) Estimation of mean monthly solar global radiation as a function of temperature. Agric For Meteorol 100:231–241

Myers DR (2005) Solar radiation modeling and measurements for renewable energy applications: data and model quality. Energy 30:1517–1531

Peel MC, Finlayson BL, McMahon TA (2007) Updated world map of the Koppen-Geiger climate classification. Hydrol Earth Syst Sci 11(5): 1633–1644

Romo J, Arteaga R (1983) Meteorología Aplicada. Universidad Autónoma de Chapingo. 442 pp

Salima G, Chavula GMS (2012) Determining angstrom constants for estimating solar radiation in Malawi. Int J Geosci 3:391–397

Spencer JW (1971) Fourier series representation of the position of the Sun. Search 2(5):172
Thorton PE, Running SW (1999) An improved algorithm for estimating incident daily solar radiation from measurements of temperature, humidity and precipitation. Agric For Meteorol 93:211–228
Vecam D (2011) Measurement and comparison of solar radiatoion estimation for Izmir/Turkey. Izmir Institute of Technology Case. Master of Science, Izmir Institute of Technology
Woodwell GM (1967) Radiation and the patterns of nature. Science 156: 461–470